AXIAL SYMMETRY AND ROTATION IN THE SiO MASER SHELL OF IK TAURI

D. A. BOBOLTZ

US Naval Observatory, 3450 Massachusetts Avenue, NW, Washington, DC 20392-5420; dboboltz@usno.navy.mil

AND

P. J. DIAMOND

Jodrell Bank Observatory, University of Manchester, Macclesfield, Cheshire SK11 9DL, UK; pdiamond@jb.man.ac.uk

ABSTRACT

We observed $v = 1, J = 1$–0 43 GHz SiO maser emission toward the Mira variable IK Tauri (IK Tau) using the Very Long Baseline Array (VLBA). The images resulting from these observations show that SiO masers form a highly elliptical ring of emission approximately 58×32 mas with an axial ratio of 1.8:1. The major axis of this elliptical distribution is oriented at a position angle of $\sim 59°$. The line-of-sight velocity structure of the SiO masers has an apparent axis of symmetry consistent with the elongation axis of the maser distribution. Relative to the assumed stellar velocity of 35 km s^{-1}, the blue- and redshifted masers were found to lie to the northwest and southeast of this symmetry axis, respectively. This velocity structure suggests a northwest–southeast (NW–SE) rotation of the SiO maser shell with an equatorial velocity, which we determine to be ~ 3.6 km s^{-1}. Such a NW–SE rotation is in agreement with a circumstellar envelope geometry invoked to explain previous H$_2$O and OH maser observations. In this geometry, H$_2$O and OH masers are preferentially created in a region of enhanced density along the NE–SW equator orthogonal to the rotation/polar axis suggested by the SiO maser velocities.

Subject headings: circumstellar matter — masers — radio lines: stars — stars: AGB and post-AGB — stars: individual (IK Tauri)

1. INTRODUCTION

The star IK Tau, also know as NML Tau (Neugebauer et al. 1965), is an extremely red Mira variable with an unusually late spectral type ranging from M8.1 to M11.2 (Wing & Lockwood 1973). The period of IK Tau is ~ 470 days, as determined from infrared photometry measurements at 1 μm (Wing & Lockwood 1973) and at 11 μm (Hale et al. 1997). Olofsson et al. (1998) computed a distance of 250 pc from integrated visual, near-infrared, and *IRAS* data using the period-luminosity relationship of Whitelock et al. (1994). This distance is consistent with the 270 pc determined by Hyland et al. (1972) using infrared flux measurements and an assumed long-period variable maximum luminosity of 10^{-4}. Mass-loss rates estimated from the CO($J = 1$–0) line range from 5.1×10^{-6} $M_\odot$ yr^{-1} (Knapp & Morris 1985) to 2.4×10^{-6} $M_\odot$ yr^{-1} (Olofsson et al. 1998).

Long-period variables such as IK Tau often exhibit circumstellar maser emission in one or more molecular species (i.e., OH, H$_2$O, or SiO). IK Tau is one such star that has maser emission in all three species. The OH and H$_2$O masers toward IK Tau have been mapped using connected element and radio-linked interferometers (Lane et al. 1987; Bowers et al. 1989, 1993; Yates & Cohen 1994; Bains et al. 2003), revealing the structure of the circumstellar envelope (CSE) on both large scales ($2''$–$4''$ traced by the OH masers) and intermediate scales (200–350 mas traced by the H$_2$O masers). Such studies have been useful in determining the structure of the CSE on these scales. The SiO masers, which lie close to the star, provide a unique probe of the morphology of the CSE and the velocity of the gas in a region just a few stellar radii from the photosphere. Previous very long baseline interferometry (VLBI) observations of long-period variables have demonstrated the various morphologies that exist in the SiO maser region. Some stars exhibit ring-like SiO maser distributions (Diamond et al. 1994; Diamond & Kemball 1998; Cotton et al. 2004), while others (e.g., NML Cyg)

show more elliptical distributions (Boboltz & Marvel 2000). Previous SiO maser studies have also revealed the velocity structure of the nearby CSE to be complex, showing elements of contraction (Boboltz et al. 1997), expansion (Diamond & Kemball 2003), and even rotation (Boboltz & Marvel 2000; Hollis et al. 2001; Sánchez Contreras et al. 2002; Cotton et al. 2004). In this article, we present the results from our VLBI observations of the SiO maser emission toward the long-period variable IK Tau. We discuss how these observations fit into the overall picture of the CSE as traced by the various maser species and the possibility of axial symmetry and rotation in the envelope of IK Tau.

2. OBSERVATIONS AND REDUCTION

We observed the $v = 1, J = 1$–0 SiO maser emission toward IK Tau ($\alpha = 03^h53^m28^s.8$, $\delta = 11°24'22''.4$ [J2000]) on 1996 April 5 from 20:00 to 24:00 UT. Based on a period of 470 days (Wing & Lockwood 1973; Hale et al. 1997) and a maximum at JD 2,439,440 (Wing & Lockwood 1973), the stellar phase of IK Tau was ~ 0.85 during the epoch of our observations. IK Tau and a continuum calibrator (0423-013) were observed using the 10 stations of the VLBA plus a single antenna of the Very Large Array (VLA). Both the VLBA and VLA are operated by the National Radio Astronomy Observatory (NRAO).[1] A reference frequency of 43.122027 GHz was used for the $v = 1, J = 1$–0 SiO transition. Data were recorded in dual circular polarization using a single 4 MHz (27.8 km s^{-1}) band centered on the local standard of rest (LSR) velocity of 34.0 km s^{-1}. System temperatures and point source sensitivities were on the order of ~ 150 K and ~ 11 Jy K^{-1}, respectively.

Report Documentation Page

Form Approved
OMB No. 0704-0188

Public reporting burden for the collection of information is estimated to average 1 hour per response, including the time for reviewing instructions, searching existing data sources, gathering and maintaining the data needed, and completing and reviewing the collection of information. Send comments regarding this burden estimate or any other aspect of this collection of information, including suggestions for reducing this burden, to Washington Headquarters Services, Directorate for Information Operations and Reports, 1215 Jefferson Davis Highway, Suite 1204, Arlington VA 22202-4302. Respondents should be aware that notwithstanding any other provision of law, no person shall be subject to a penalty for failing to comply with a collection of information if it does not display a currently valid OMB control number.

1. REPORT DATE	2. REPORT TYPE	3. DATES COVERED
01 JUN 2005	**N/A**	**-**

4. TITLE AND SUBTITLE	5a. CONTRACT NUMBER
Axial Symmetry and Rotation in the SiO Maser Shell of IK Tauri	5b. GRANT NUMBER
	5c. PROGRAM ELEMENT NUMBER

6. AUTHOR(S)	5d. PROJECT NUMBER
	5e. TASK NUMBER
	5f. WORK UNIT NUMBER

7. PERFORMING ORGANIZATION NAME(S) AND ADDRESS(ES)	8. PERFORMING ORGANIZATION REPORT NUMBER
U.S. Naval Observatory 3450 Massachusetts Avenue, N.W. Washington, D.C. 20392-5420	

9. SPONSORING/MONITORING AGENCY NAME(S) AND ADDRESS(ES)	10. SPONSOR/MONITOR'S ACRONYM(S)
	11. SPONSOR/MONITOR'S REPORT NUMBER(S)

12. DISTRIBUTION/AVAILABILITY STATEMENT
Approved for public release, distribution unlimited

13. SUPPLEMENTARY NOTES
The original document contains color images.

14. ABSTRACT

15. SUBJECT TERMS

16. SECURITY CLASSIFICATION OF:			17. LIMITATION OF ABSTRACT	18. NUMBER OF PAGES	19a. NAME OF RESPONSIBLE PERSON
a. REPORT **unclassified**	b. ABSTRACT **unclassified**	c. THIS PAGE **unclassified**	**UU**	**7**	

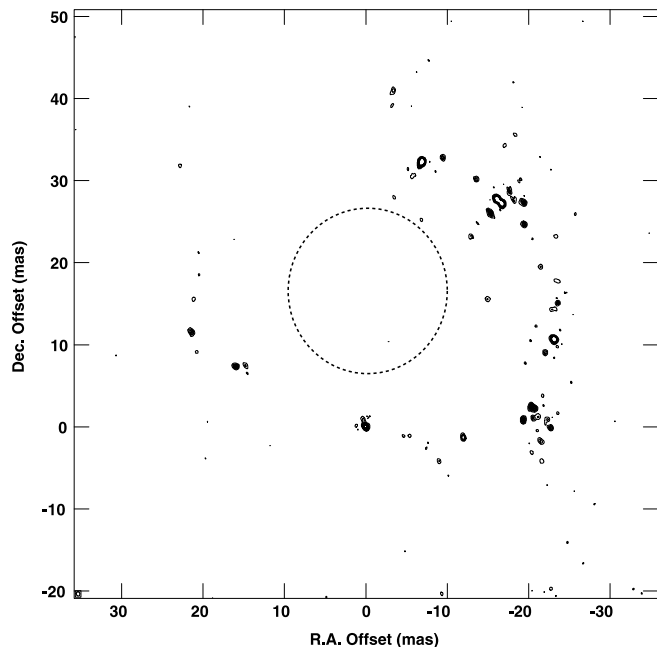**Standard Form 298 (Rev. 8-98)**
Prescribed by ANSI Std Z39-18

FIG. 1.—Total intensity VLBI images of the $v = 1$, $J = 1-0$ SiO maser emission toward IK Tau integrated over the LSR velocity range from +28.8 to +41.6 km s^{-1}. Contour levels are -3%, -1.5%, 1.5%, 3%, 5%, 10%, 20%, 40%, and 80% of the peak integrated flux density of 49.9 Jy beam^{-1}. The synthesized beam is 0.54×0.41 mas at a position angle of $14°.1$. The dashed circle represents a stellar uniform disk diameter of 20.2 mas from Monnier et al. (2004). The location of the stellar disk is conjecture.
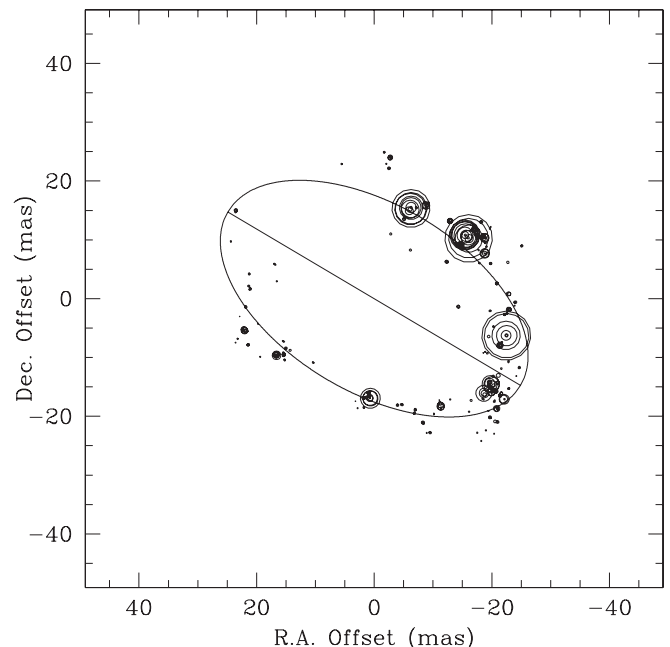

FIG. 2.—Maser spot map as derived from the two-dimensional Gaussian fits to masers in each plane in the image cube. Point sizes are proportional to the logarithm of the flux density. The ellipse indicates a flux-density-weighted least-squares fit to the maser distribution.

The data were correlated at the VLBA correlator operated by the NRAO in Socorro, New Mexico. Auto- and cross-correlation spectra consisting of 128 channels with channel spacings of 31.25 kHz (~ 0.2 km s^{-1}) were produced by the correlator. Calibration was performed using the Astronomical Image Processing System (AIPS) maintained by NRAO. Total intensity (Stokes I) data were calibrated in accordance with the procedures outlined in Diamond (1989). The bandpass response was determined from scans on the continuum calibrator and used to correct the target source data. The time-dependent gains of all antennas relative to a reference antenna were determined by fitting a total-power spectrum (from the reference antenna with the target source at a high elevation) to the total-power spectrum of each antenna. The absolute flux density scale was established by scaling these gains by the system temperature and gain of the reference antenna. Errors in the gain and pointing of the reference antenna and the atmospheric opacity contribute to the error in the absolute amplitude calibration, which is accurate to about 15%–20%. Residual group delays were determined by performing a fringe fit to the continuum calibrator sources and were applied to the spectral line data. Residual fringe-rate solutions were obtained by fringe fitting a strong reference feature in the channel at $V_{LSR} = 36.2$ km s^{-1} and were applied to all channels in the spectrum. An iterative self-calibration and imaging procedure was performed to map the reference channel at 36.2 km s^{-1}. The resulting phase solutions were applied to all channels in the band.

Images of the SiO maser emission consisting of 1024×1024 pixels ($\sim 72 \times 72$ mas) were generated using a synthesized beam of 0.54×0.41 mas in natural weighting. Images were produced for spectral channels from 28.8 to 41.6 km s^{-1}, forming an image cube of 60 planes. Off-source rms noise estimates in the spectral channel images range from 10 mJy beam^{-1} in planes with weak or no maser emission to 80 mJy beam^{-1} in dynamic-

range–limited planes containing strong ($\gtrsim 15$ Jy beam^{-1}) maser emission. Figure 1 shows the total intensity contour map of the 43.1 GHz SiO masers integrated over the LSR velocity range above. The dashed circle in the figure represents the stellar photosphere with a diameter of 20.2 mas. This diameter was determined from a uniform disk (UD) diameter fit to combined Keck aperture-masking data and Infrared Optical Telescope Array (IOTA) data in the near-infrared (Monnier et al. 2004). It is apparent from Figure 1 that the SiO masers toward IK Tau form an elongated ring roughly 58×32 mas across oriented in the northeast–southwest (NE–SW) direction. If the star is assumed to be in the center of the distribution, maser distances range from ~ 1.6 to 2.8 stellar radii.

In order to identify and parameterize maser components, two-dimensional Gaussian functions were fitted to the emission in each spectral (velocity) channel using the AIPS task SAD. Image quality was assessed using the off-source rms noise and the deepest negative pixel in the image. A cutoff, above which emission features were fit, was conservatively set to the greater of 10 σ_{rms} or 80% of the absolute value of the deepest negative pixel in the plane. Errors reported by SAD were based on the source size divided by twice the signal-to-noise ratio (S/N) in the image and ranged from 5 μas for features with high S/N to 371 μas for features with lower S/N. The emission features identified by SAD are represented by the circles in Figure 2. In the figure, point sizes are proportional to the logarithm of the fitted flux density, which ranged from 0.2 to 18.3 Jy. Comparing Figures 1 and 2, we see that the identified features accurately represent the emission summed over all velocity channels in the image cube.

3. RESULTS AND DISCUSSION

3.1. Axial Symmetry in the CSE of IK Tau

Figures 1 and 2 show that the distribution of the 43.1 GHz SiO maser emission toward IK Tau was clearly not circularly symmetric during the epoch of our observations. Instead, the

distribution appears to be elongated along an axis running from the northeast to the southwest in the images. We characterized this morphology by performing a least-squares fit of an ellipse to the distribution of masers weighted by the flux density of each component. The resulting ellipse is plotted in Figure 2. The lengths of the semimajor and semiminor axes were found to be 29 and 16 mas, respectively, with the semimajor axis of the ellipse oriented at $59°$ measured east of north. At the assumed distance to IK Tau of 250 pc, the distribution of SiO masers is approximately 15×8 AU. The SiO maser distributions of $\lesssim 20$ late-type stars have previously been imaged with angular resolutions provided by VLBI (e.g., Cotton et al. 2004; Diamond & Kemball 2003; Sánchez Contreras et al. 2002; Hollis et al. 2001; Boboltz & Marvel 2000; Diamond et al. 1994). Of these stars, IK Tau, with an axial ratio of $\sim 1.8{:}1$, appears to have one of the most elongated SiO rings yet observed.

As mentioned previously, Monnier et al. (2004) were able to separate the near-infrared stellar and dust contributions and determine a UD diameter of 20.2 mas for the photosphere of IK Tau. However, they found that the longest (27 m) IOTA baseline data were inconsistent with this fit, and the data were thus ignored. Possible explanations for this deviation are departures from uniform photospheric brightness (e.g., stellar hot spots or extended molecular emission) or the presence of a binary companion (Monnier et al. 2004).

The circumstellar dust shell, typically outside the SiO maser region, has been observed for IK Tau using long-baseline interferometers operating at mid-infrared (Danchi et al. 1994; Hale et al. 1997) and near-infrared (Monnier et al. 2004) wavelengths. Hale et al. (1997) found that their Infrared Spatial Interferometer (ISI) 11 μm visibilities were best fit by three spherically symmetric concentric dust shells. However, Monnier et al. (2004) state that their Keck-IOTA data, which include multiple late-type stars, suggest that the popular strategy of incorporating multiple spherically symmetric shells to model deviations from simple uniform outflow might be misguided, and that clumpiness and global asymmetry should be considered more seriously. In fact, Monnier et al. (2004) report that the visibility data for IK Tau show signs of asymmetries for the dust shell, but the data are not of sufficient quality to make a definitive determination.

Beyond the regions of the SiO masers and circumstellar dust shell, there is evidence for axisymmetric structures in the CSE of IK Tau. On large angular scales, Bowers et al. (1989) found that the 1612 MHz OH masers form an elongated ring $\sim 3{.}^{\prime\prime}5 \times 2{.}^{\prime\prime}3$ with a NW–SE orientation of the long axis. The axisymmetry is especially apparent at high velocities ($V > 45$ km s^{-1}) where nearly all of the emission originates to the SE and NW of the star. Observations of the 22 GHz H$_2$O masers with the VLA (Lane et al. 1987; Bowers et al. 1993) and the Multi Element Radio Linked Interferometer Network (MERLIN; Yates & Cohen 1994; Bains et al. 2003) show similar axial symmetry with respect to the NW–SE direction. VLA observations by Lane et al. (1987) show that the low-velocity masers have a ringlike distribution, while the high-velocity masers have a flattened distribution with a NW–SE orientation. The overall size of the shell was roughly 330 mas. The VLA data of Bowers et al. (1993) show the H$_2$O maser distribution to be $\sim$220 mas across, with a similar elongation in the NW–SE direction. The MERLIN images of Bains et al. (2003) show bright blue- and redshifted emission distributed over an elliptical region approximately 100×200 mas superimposed on a fainter spherical region of emission from all spectral channels.

The observed NE–SW orientation for the elliptical SiO maser distribution is roughly orthogonal to elongations of the H$_2$O and OH maser distributions. Bowers et al. (1989) suggest that the axisymmetric structures seen in the OH and H$_2$O maser shells for certain late-type stars are a result of the density distribution of gas and dust in the CSE. They conclude that the density distribution is latitude dependent, with the total density decreasing as the latitude increases from the rotationally defined equatorial plane. In stars in which both the OH and H$_2$O masers are axially symmetric (e.g., IK Tau) Bowers et al. (1989) suggest that the distributions should be aligned parallel along the equatorial plane, since the density enhancement is conducive to the formation of the H$_2$O masers (assuming these masers are collisionally pumped), and since the OH masers are the result of the photodissociation of the H$_2$O by the surrounding UV radiation. Yates & Cohen (1994) state that their MERLIN data are also supportive of a NW–SE equator for IK Tau with the brightest H$_2$O masers observed along this axis as expected. Assuming this NW–SE axis is parallel to the equator of IK Tau, as suggested by the OH and H$_2$O maser observations, then the elongation we observe in the SiO maser distribution is along an axis roughly perpendicular to the equator and possibly parallel to the polar axis of the star. The importance of this geometry will become apparent in the discussion of the velocity structure of the SiO masers in the next section.

3.2. *Velocity Structure of the* SiO *Masers*

The line-of-sight (LOS) velocity information derived from our VLBA data is shown in Figure 3. The top panel shows the spectrum of SiO maser emission from 28 to 42 km s^{-1} color coded by LOS velocity in increments of 1.5 km s^{-1}. The bottom panel of Figure 3 shows the SiO masers plotted in the same velocity color coding as the top panel, with the color of the maser spot representing its corresponding velocity in the spectrum. It is apparent from the figure that there is a symmetry axis for the velocity structure of the SiO maser emission toward IK Tau, with the northwestern side of the shell dominated by blueshifted masers (relative to the assumed stellar velocity of 35 km s^{-1}) and the southeastern side of the shell dominated by redshifted masers. Such velocity distributions in which blue- and redshifted SiO masers occur on opposite sides of the star have previously been observed for NML Cyg (Boboltz & Marvel 2000), R Aqr (Hollis et al. 2001; Cotton et al. 2004), and OH 231.8+4.2 (Sánchez Contreras et al. 2002). For NML Cyg and R Aqr, the maser velocity distributions suggested rotation of their respective maser shells. In the case of OH 231.8+4.2, Sánchez Contreras et al. (2002) concluded that the maser distribution could be modeled by a rotating, contracting torus of emission.

The ringlike distributions typically observed in VLBA studies of SiO masers indicate that the masers are amplified in a direction perpendicular to the radial direction (i.e., tangential amplification; Diamond et al. 1994). This amplification occurs along the longest path lengths parallel to the observer's LOS. Assuming this is the case for IK Tau, then the velocity structure shown in Figure 3 suggests a NW–SE rotation of the maser shell with the axis of rotation near the elongation axis of the distribution. Such a rotation axis is in agreement with a NE–SW equator for IK Tau, as indicated by the previous OH and H$_2$O maser observations mentioned above.

Rotation is not a new concept with regard to the masers in the CSE of IK Tau. Bowers et al. (1989) considered models with radial expansion combined with Keplerian rotation to explain the axisymmetric geometries observed for the 1612 MHz OH masers. They concluded that although rotation could not unequivocally be ruled out, the data did not support rotation as a primary component in the kinematics of the OH shell. Additionally,
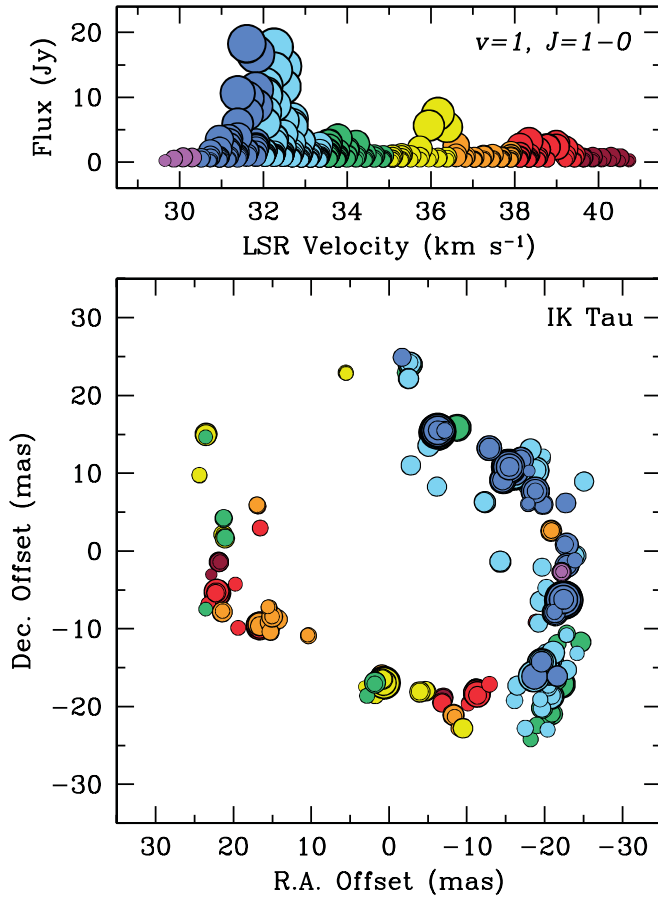
FIG. 3.—Structure of the SiO maser emission toward IK Tau as measured by the two-dimensional Gaussian fit to the masers in the VLBI channel maps. *Top panel*: Spectrum formed by plotting component flux density vs. velocity, color coded in 1.5 km s^{-1} velocity increments from redward (*left*) to blueward (*right*). *Bottom panel*: Plots the spatial and velocity distribution of the masers. The color of each point represents the corresponding velocity bin in the spectrum, and the size of each point is proportional to the logarithm of the flux density. Errors in the positions of the features are smaller than the data points.

Bowers et al. (1993) found that the plot of radius versus velocity for their H_2O maser data was reminiscent of models of accelerating or axisymmetric outflow with a possible rotational component.

To better characterize the velocity structure of the SiO emission, we investigated a number of models with velocity components including rotation and expansion/contraction. Modeling the three-dimensional velocity structure of the SiO masers toward IK Tau is complicated by the elliptical distribution of the masers and by a lack of knowledge of the shell structure along the observer's LOS. The elliptical distribution of the masers could be modeled by either an ellipsoidal shell or an inclined torus similar to that of Sánchez Contreras et al. (2002). We chose an ellipsoidal shell, based on the assumption that the masers are tangentially amplified and the fact that nearly a full ring of emission is observed. In the case of a torus with tangential amplification, one would expect to see only two regions of emission on opposite sides of the star, as was observed by Sánchez Contreras et al. (2002). Models developed for IK Tau are based on a prolate spheroid with the long axis oriented at a position angle of 59° (as suggested by the elliptical fit shown in Fig. 2). Since the true three-dimensional shape of the maser shell is unknown, the axis of the ellipsoidal model along the observers LOS was assumed to be the same size as the minor axis of the

model in the plane of the sky. Additionally, the inclination of the ellipsoid was assumed to be zero.

The models were compared "by eye" to the actual data to determine how well they reproduced the true maser spatial and velocity distributions. To make the comparison easier, we plotted the data and the models in a manner similar to that presented in Hollis et al. (2001), with three different views. Figure 4 shows the VLBA data plotted in the three panels on the left. The top panel plots the maser distribution with the same color coding as that of Figure 3, along with a set of axes (X, Z) determined from the elliptical fit of Figure 2. The middle panel plots the component LOS velocity versus its position along the equatorial (X) axis. The bottom panel plots the component LOS velocity versus its position along the polar (Z) axis. The right three panels of Figure 4 plot the equivalent distributions derived from the model.

The size and shape of the model shell (i.e., major axis, minor axis, and shell thickness) were chosen to approximate the spatial distribution of the SiO masers as seen in Figure 3 and the top-left panel of Figure 4. Maser velocities were first modeled with a general form of rotation given by

$$V(r) \propto Ar^p. \qquad (1)$$

It quickly became apparent that models including only rotation do not sufficiently approximate the maser data. In the middle-left panel of Figure 4, we see that there is a significant variation in position along the X-axis for masers with small (<2 km s^{-1}) LOS velocities. It is this spread in position for low-velocity points that is difficult to model assuming only rotation. For example, solid-body rotation ($p = 1$) yields a simple linear variation of LOS velocity with position along the X-axis, regardless of distance along the Z-axis. Keplerian rotation ($p = -0.5$) gives a greater variation in X-axis position for higher velocity masers; however, at lower velocities the positions are still confined to a narrow region in the V_{LOS} versus X plot (see Fig. 3 of Hollis et al. 2001).

One way to produce the observed spread in position at small LOS velocities is to add an expansion term to the equation describing the motion of the masers in the shell. The LOS velocity for an elliptical shell that is in rotation and also has a component of constant velocity expansion, V_{exp}, can be written

$$V(r)_{LOS} = V_{LPV} + \sqrt{\frac{GM}{r^q}} \cos \theta \cos \phi + V_{exp} \sin \theta \cos \phi, \qquad (2)$$

where the rotational term is similar to that of Hollis et al. (2001); note that the exponent q allows for sub- or super-Keplerian rotation. In equation (2), M represents the mass of the star, V_{LPV} is the stellar velocity, the angle θ is measured in the equatorial plane of the shell, and the angle ϕ is the latitudinal coordinate of the shell. Since the mass of IK Tau is unknown, 1 $M_\odot$ was assumed for the model. The stellar velocity, V_{LPV}, was assumed to be 35 km s^{-1}, consistent with velocities determined from the midpoints of the spectra of the 1612 MHz OH masers, 33.2 km s^{-1} (Bowers et al. 1989), and the H_2O masers, 35.4 km s^{-1} (Bowers et al. 1993). Similar to the models of Humphreys et al. (1996, 2002), maser gain length was approximated by considering the distance along the path in which the LOS velocity changes by less than 3 times the Doppler width of the line. Amplification becomes negligible for velocity shifts greater than this limit (Humphreys et al. 1996, 2002). For SiO we estimated a Doppler line width $\Delta V_D \approx 1$ km s^{-1} for a typical temperature of 1500 K in the SiO maser region (Doel et al. 1995). The maser gain length was further
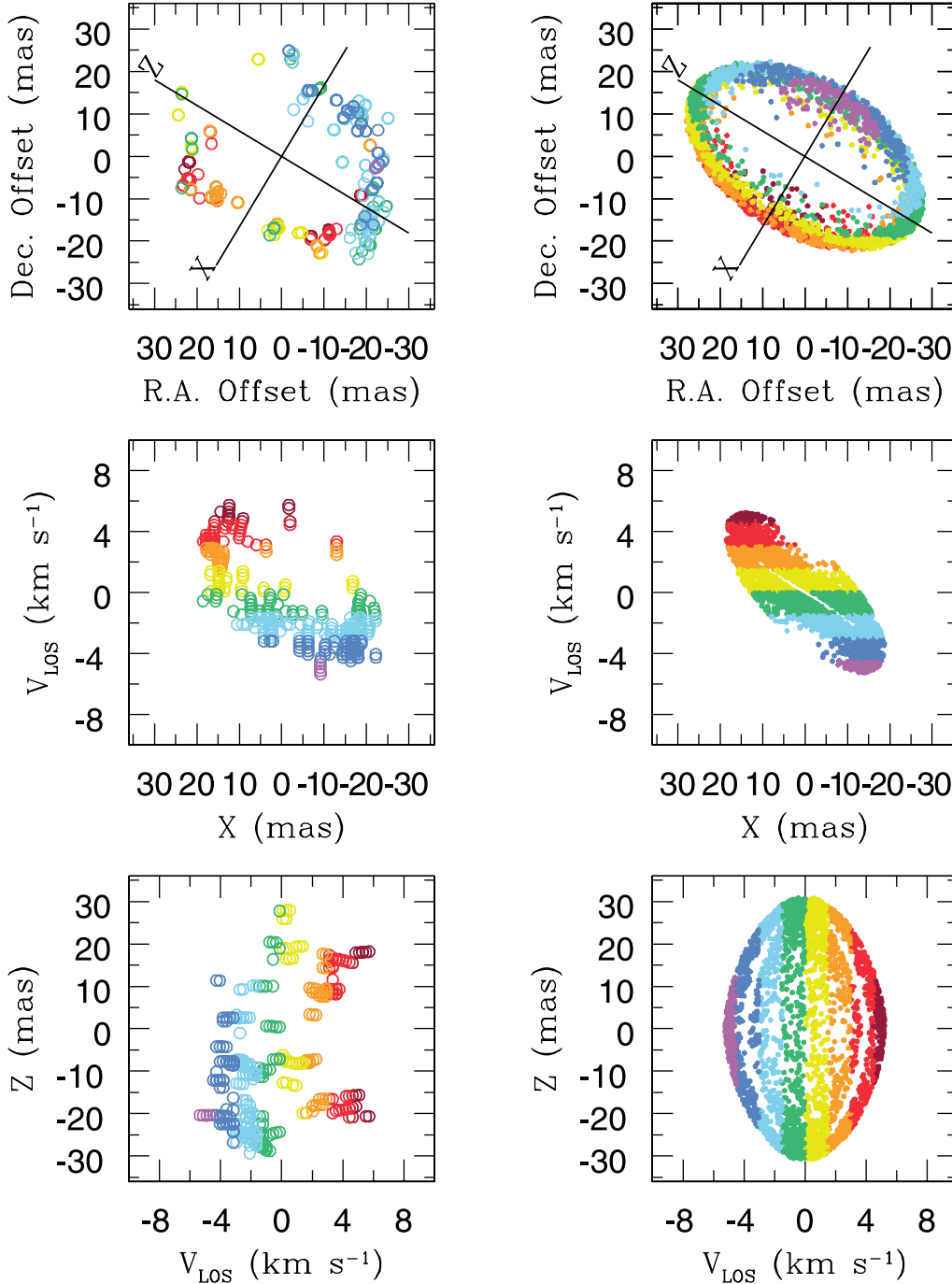
Fig. 4.—Side-by-side color-coded plots of the VLBA data (*left*) and the ellipsoidal shell model (*right*). Velocity color coding is the same as for Fig. 3, except that the assumed stellar velocity of IK Tau ($V_{LPV} = 35$ km s^{-1}) has been subtracted. The top panels show the orientation of the VLBA data (*left*) and model (*right*) distributions on the sky and the assumed rotational and equatorial axes, Z and X, respectively, with the rotation axis at P.A. $= 59°$. The top left panel is analogous to the Fig. 3 bottom panel. The middle and bottom panels show the LOS velocities plotted against the X and Z axes of the distribution, respectively, for both the VLBA data (*left*) and the model (*right*).

constrained to be greater than the minimum path length of 10^{13} cm necessary for SiO maser emission (Elitzur 1982), and to be less than or equal to the physical LOS path length through the shell.

In practice, a random point is chosen within the region determined by the geometric parameters of the shell (i.e., size, orientation, and thickness). The LOS velocity for this point is computed from equation (2). From this point, distances forward and backward along the observer's LOS are computed, for which the LOS velocity changes by 1.5 times the Doppler line width. Thus, we have a line of points, with the chosen random point as

the center, for which $V(r)_{LOS}$ is within 3 times the Doppler line width. If both ends of the line reside within the maser shell and the total length of the line is greater than the minimum path length required for maser emission, then the center point is kept and is color coded according to its $V(r)_{LOS}$. Otherwise, the point is rejected. In this manner, the model builds up a distribution of points mapping both the structure of the shell and the maser velocity distribution.

The model shown in Figure 4 is meant to provide a qualitative match to the IK Tau SiO maser distribution. The parameters

TABLE 1
ELLIPSOIDAL SHELL MODEL PARAMETERS

Parameter	Value
Shell Geometry:	
Semiminor axis, A_0	16 mas
Semimajor axis, B_0	28 mas
Shell thickness	2.6 mas
Position angle...	$59°$
Inclination, i	$0°$
Distance..	250 pc
Stellar mass, M	$1\ M_\odot$
Stellar velocity, V_{LPV}	35.0 km s^{-1}
Minimum maser path length	1×10^{13} cm
Doppler line width, ΔV_D...............................	1.0 km s^{-1}
Expansion velocity, V_{exp}	3.5 km s^{-1}
Exponent, q	1.09

for the model are presented in Table 1. Inner distances of 16 and 28 mas were used for the semiminor, A_0, and semimajor, B_0, axes, respectively, with a shell thickness of 3 mas. As mentioned previously, the position angle for the ellipse was set to $59°$. The model is not particularly sensitive to this angle, and changes of $\lesssim 5°$ do not alter the results significantly. The two parameters that affect the velocity structure are the exponent q and the expansion velocity V_{exp}. Through an iterative process of adjusting parameters and qualitatively comparing the model to the data, values of $q = 1.09$ and $V_{exp} = 3.5$ km s^{-1} were determined. Coincidentally, the value for q is equivalent to that found for R Aqr by Hollis et al. (2001). As in the model for R Aqr, the model for IK Tau is sensitive to small (~ 0.01) variations in the value of q. Unlike the R Aqr case, the mass of IK Tau is not well constrained, and variations in the assumed value for M could allow for slight variations in the value of q. To produce a model similar to that shown in Figure 4 with pure Keplerian motion ($q = 1$) would require a stellar mass of $M \approx 0.1\ M_\odot$. Similarly, the model is sensitive to the expansion velocity V_{exp}. Changes on the order of ~ 1.0 km s^{-1} produce significant changes in the velocity distributions of the masers.

Additionally, there is a trade-off between the model expansion velocity and the quenching of the masers caused by the Doppler line width limitation. Larger values for V_{exp} tend to spread the distribution in the middle panel of the model plot, but only if ΔV_D is increased to allow the greater change in velocity and resulting longer gain lengths. The longer path lengths, in turn, create more masers in front of and behind the star, a characteristic that is clearly not evident in these or any other SiO maser observations of which we are aware. As the top right panel of Figure 4 shows, the density distribution of masers resulting from the path length considerations is characterized by tangentially amplified masers along the limb of the shell. In order to limit maser emission along the LOS to the star, the maser shell thickness must be less than or approximately equal to the maser minimum path length. Since we assumed a minimum maser path length of 10^{13} cm (~ 2.7 mas at the assumed distance to IK Tau), the shell thickness was set to 2.6 mas. Without increasing the minimum required path length, increasing the maser shell thickness will produce masers along the LOS to the star, thus filling in the distribution in the top-right panel of Figure 4.

The expansion velocity $V_{exp} = 3.5$ km s^{-1} used in the model is consistent with observational evidence as found in proper-motion studies of SiO masers. Boboltz et al. (1997) measured the proper motions of the SiO masers toward R Aqr and found

an overall infall of the masers (shell contraction) with a velocity of ~ 4 km s^{-1} over stellar phases $\phi = 0.78-1.04$. Diamond & Kemball (2003), in an extensive study of the Mira variable TX Cam, determined the dominant mode to be expansion of the SiO masers, with radial proper-motion magnitudes of $\sim 5-10$ km s^{-1} between stellar phases $\phi \approx 0.5-1.5$.

From our single epoch of SiO maser observations, it is difficult to tell whether the model expansion term represents a physical expansion or contraction of the maser shell. This is because both expansion and contraction produce nearly identical distributions in the both the middle- and lower-right panels of Figure 4. The only difference between a positive or negative expansion term is observable in the top-right panel of Figure 4. For example, if we consider only rotation of the shell, we find that all of the redshifted masers occur along the positive X-axis (the SE side of the shell), and all of the blueshifted masers occur along the negative X-axis (NW side of the shell), and the velocities are symmetric about the plane of the sky. The addition of a positive expansion term (as was done for our model) serves to rotate the blueshifted velocities out of the plane of the sky toward the front of the shell closest to the observer and the redshifted velocities away from the observer. However, the actual masers are still confined to a region around the plane of the sky; thus, the shift in the velocity structure is most easily observed near the poles along the Z-axis where we see in the top-right panel of Figure 4 that some low-velocity blueshifted masers (*green*) have been shifted toward the positive X-axis. Contraction of the shell has the opposite effect, rotating the redshifted velocity structure out of the plane toward the front of the shell and the blueshifted velocities toward the back of the shell. It is practically impossible to tell from our maser data whether expansion or contraction is the case for the IK Tau shell. There seems to be a slight preference for blueshifted masers in general and a tendency for some blueshifted masers along the positive X-axis in the top-left panel of Figure 4, but this is highly dependent on the assumed stellar velocity of 35 km s^{-1} and the choice of position angle for the major axis of the ellipse.

The maser shell rotational velocities produced in the model are not considered extraordinary. The equatorial velocity at the distance of the mean semiminor axis of 16 mas is ~ 3.6 km s^{-1} with a corresponding rotational period of ~ 33 yr. At the UD photospheric distance of 10.1 mas, the equatorial velocity is ~ 4.6 km s^{-1} with a corresponding rotational period of ~ 16 yr. These rotational velocities are consistent with observational measurements for R Aqr ($\sim 3-5$ km s^{-1}; Hollis et al. 2001; Cotton et al. 2004) and slightly lower than measurements for NML Cyg (~ 11 km s^{-1}; Boboltz & Marvel 2000) and OH 231.8+4.2 ($\sim 7-10$ km s^{-1}; Sánchez Contreras et al. 2002). Significant stellar rotation velocities (10–100 s of km s^{-1}) during the asymptotic giant branch (AGB) phase have been invoked in theoretical studies of chemical mixing and the nucleosynthesis of heavy elements in convective envelopes (Langer et al. 1999; Herwig et al. 2003; Siess et al. 2004). Stellar rotation is also a factor in models describing the shaping of bipolar and elliptical planetary nebulae, and García-Segura et al. (1999) propose that AGB stars above $\sim 1.3\ M_\odot$ can spin up their extended circumstellar envelopes to rotational speeds on the order of a km s^{-1}. Stellar rotation velocities of $\sim 3-7$ km s^{-1} are used in such models, which result in equatorial density enhancements and eventually bipolar nebulae (García-Segura et al. 1999). Interestingly, the collective maser observations of IK Tau, which suggest rotation, axial symmetry, and equatorial density enhancement, may be indicating that IK Tau is on its way to becoming such a bipolar planetary nebula.

4. SUMMARY

We have imaged the $v = 1$, $J = 1$–0 SiO maser emission toward the Mira variable IK Tau. We find that the SiO masers are distributed in an elongated ring roughly 58×32 mas (15×8 AU at the adopted distance of 250 pc) with the major axis of the ellipse at a position angle of $\sim 59°$. The NE–SW elongation of the SiO maser distribution is roughly perpendicular to the NW–SE symmetry axis previously determined for the H$_2$O and OH maser distributions. This elongation axis also provides an axis of symmetry for the LOS velocity structure of the SiO masers. Masers having velocities blueshifted with respect to the assumed center velocity of 35 km s^{-1} were found to lie on the northwestern side of the shell, while the southeastern side of the shell is dominated by redshifted SiO masers. Under the assumption of tangentially amplified masers, this velocity distribution implies a NW to SE rotation of the SiO shell about a NE–SW rotation/polar axis. Such a polar axis would be in agreement with models invoked to explain the H$_2$O and OH maser geometries, which suggest a NW–SE equator for IK Tau.

The inherent transient and irregular nature of SiO maser emission in the atmospheres of long-period variables limits the comparison of models to a single epoch of VLBI data. However, we have attempted to approximate the IK Tau observations presented here assuming an ellipsoidal model of the SiO maser shell. We favor a model that includes both rotation of the form $V \propto 1/r^{1.09}$ and constant-velocity expansion/contraction as a representation of the velocity field in the CSE of IK Tau at the distance of the SiO maser shell. This model appears to reproduce the global characteristics of the observed SiO masers in terms of structure and velocity distribution. A multiepoch VLBI monitoring program to determine the SiO maser proper motions could verify this scenario and would greatly clarify our understanding of the CSE of IK Tau.

REFERENCES

Bains, I., Cohen, R. J., Louridas, A., Richards, A. M. S., Rosa-González, D., & Yates, J. A. 2003, MNRAS, 342, 8
Boboltz, D. A., Diamond, P. J., & Kemball, A. J. 1997, ApJ, 487, L147
Boboltz, D. A., & Marvel, K. B. 2000, ApJ, 545, L149
Bowers, P. F., Claussen, M. J., & Johnston, K. J. 1993, AJ, 105, 284
Bowers, P. F., Johnston, K. J., & de Vegt, C. 1989, ApJ, 340, 479
Cotton, W. D., et al. 2004, A&A, 414, 275
Danchi, W. C., Bester, M., Degiacomi, C. G., Greenhill, L. J., & Townes, C. H. 1994, AJ, 107, 1469
Diamond, P. J. 1989, in Very Long Baseline Interferometry: Techniques and Applications, ed. M. Felli & R. E. Spencer (Dordrecht: Kluwer), 233
Diamond, P. J., & Kemball, A. J. 1998, in IAU Colloq. 164, Radio Emission from Galactic and Extragalactic Compact Sources, ed. J. A. Zensus, G. B. Taylor, & J. M. Wrobel (ASP Conf. Ser. 144; San Francisco: ASP), 245
———. 2003, ApJ, 599, 1372
Diamond, P. J., Kemball, A. J., Junor, W., Zensus, A., Benson, J., & Dhawan, V. 1994, ApJ, 430, L61
Doel, R. C., Gray, M. D., Humphreys, E. M. L., Braithwaite, M. F., & Field, D. 1995, A&A, 302, 797
Elitzur, M. 1982, Rev. Mod. Phys., 54, 1225
García-Segura, G., Langer, N., Różyczka, M., & Franco, J. 1999, ApJ, 517, 767
Hale, D. D. S., et al. 1997, ApJ, 490, 407
Herwig, F., Langer, N., & Lugaro, M. 2003, ApJ, 593, 1056

Hollis, J. M., Boboltz, D. A., Pedelty, J. A., White, S. M., & Forster, J. R. 2001, ApJ, 559, L37
Humphreys, E. M. L., Gray, M. D., Yates, J. A., Field, D., Bowen, G., & Diamond, P. J. 1996, MNRAS, 282, 1359
———. 2002, A&A, 386, 256
Hyland, A. R., Becklin, E. E., Frogel, J. A., & Neugebauer, G. 1972, A&A, 16, 204
Knapp, G. R., & Morris, M. 1985, ApJ, 292, 640
Lane, A. P., Johnston, K. J., Bowers, P. F., Spencer, J. H., & Diamond, P. J. 1987, ApJ, 323, 756
Langer, N., Heger, A., Wellstein, S., & Herwig, F. 1999, A&A, 346, L37
Monnier, J. D., et al. 2004, ApJ, 605, 436
Neugebauer, G., Martz, D. E., & Leighton, R. B. 1965, ApJ, 142, 399
Olofsson, H., Lindqvist, M., Nyman, L.-A., & Winnberg, A. 1998, A&A, 329, 1059
Sánchez Contreras, C., Desmurs, J. F., Bujarrabal, V., Alcolea, J., & Colomer, F. 2002, A&A, 385, L1
Siess, L., Goriely, S., & Langer, N. 2004, A&A, 415, 1089
Yates, J. A., & Cohen, R. J. 1994, MNRAS, 270, 958
Whitelock, P., Menzies, J., Feast, M., Marang, F., Carter, B., Roberts, G., Catchpole, R., & Chapman, J. 1994, MNRAS, 267, 711
Wing, R. F., & Lockwood, G. N. 1973, ApJ, 184, 873